

## Research on Nonlinear Vibration Characteristics of Spiral Bevel Gear

Nie Junfeng, \*Yu Guangbin, Song Ye, Qu Zhigang, Zheng Minli and Zhao Xingfu

*1.School of Mechanical Engineering, Harbin University of Science and Technology Heilongjiang, P.R. China, 150080*

*Corresponding Author Yu Guangbin*

*E-mail:593542635@qq.com*

### **Abstract**

*Based on the concentrated parameters theory, a 7-freedom coupled vibration dynamic model of the spiral bevel gear transmission system is established, which includes transmission error, time-varying mesh stiffness and the tooth backlash clearance. In the model, the axial vibration, the torsion oscillation of the gear pair aroused by tooth meshing force and the lateral oscillations resulting from flexional deformation of the gear shaft are taken into account. The mesh stiffness fluctuation is developed as 5-order Fourier series and the tooth backlash clearance is fitted by 7-order polynomial function. Through the Gear method, the dynamic response of the system is obtained, and the vibration characteristics are analyzed.*

**Keywords:** *vibration dynamic model, spiral bevel gear transmission system, torsion oscillation*

### **1. Introduction**

At present, most of the research on the nonlinear dynamics of gear transmission is concentrated in the study of the dynamics of spur gears. Therefore, the nonlinear dynamic model of bevel gear transmission system is established, which is based on the nonlinear factors such as backlash, time-varying mesh stiffness and so on. This research will not only provide useful theoretical basis and effective method for the design of the gear system with light weight and high efficiency. And it has important practical significance to further explore the dynamic characteristics of gear system and reduce the vibration and noise of gear system. Because of the high speed level, the dynamic characteristics of the spiral bevel gears are very important in the micro - and small - speed reduction device.

### **2. Establishment of Nonlinear Dynamic Differential Equations of the Spiral Bevel Gear System**

In this paper, the dynamic model of gear transmission system (gear, shaft and bearing) is set up by using lumped parameter method. The quality of shaft and bearing is simplified to the center of gear.

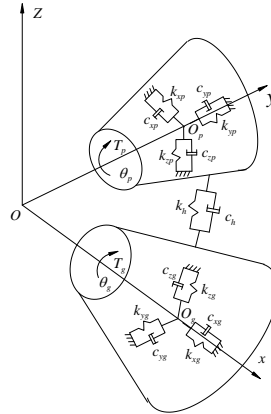


**Figure 1. The Vibration Dynamics Model of Spiral Bevel Gear**

Figure 1 shows the dynamic model of the bevel gear drive with elastic support. In this model, the axis of the two bevel gear is the origin, and the global coordinate system  $\Sigma : \{O x, y, z\}$  is established. The shaft section of the supporting two gear is treated as the middle point  $O_p$  of the tooth width of the gear.  $O_g$  moves along the three direction of the coordinates and the drive of the wheel around its axis. that is  $\{x_p, y_p, z_p, \theta_p, x_g, y_g, z_g, \theta_g\}^T$ . Two the relative displacement of the normal direction of the normal direction of the meshing point of the gear tooth surface of the bevel gear  $x_n$ . In order to analyze the force of the large gear, the coordinate system is rotated around the y axis. As shown in figure 2. Bevel gears in meshing the method to dynamic meshing force and along each coordinate direction component respectively.

$$\left. \begin{aligned} F_n &= k_m x_n + c_m \dot{x}_n \\ F_x &= -F_n (\sin \alpha_n \cos \delta_p + \cos \alpha_n \sin \beta_m \sin \delta_p) \\ F_y &= F_n (\sin \alpha_n \sin \delta_p - \cos \alpha_n \sin \beta_m \cos \delta_p) \\ F_z &= F_n \cos \alpha_n \sin \beta_m \end{aligned} \right\} \quad (1)$$

Where  $\delta_p, \delta_g$  are main passive bevel gear cone angle.  $\alpha_n$  is normal pressure angle.

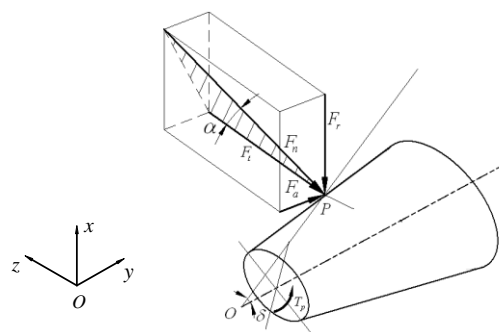


**Figure 2. Force Analysis of the Spiral Bevel Gear**

Less effect on the system due to torsion vibration, for the convenience of analysis, we ignore the torsion vibration, the spiral bevel gear transmission system with equivalent to eight degrees of freedom, but considering the gear time-varying mesh stiffness and the gear backlash coexistence of nonlinear dynamics model, Fig1 shows the spiral bevel gear transmission system vibration equation .

$$\left. \begin{aligned} m_p \ddot{X}_p + c_{xp} \dot{X}_p + k_{xp} X_p &= F_x \\ m_p \ddot{Y}_p + c_{yp} \dot{Y}_p + k_{yp} Y_p &= F_y \\ m_p \ddot{Z}_p + c_{zp} \dot{Z}_p + k_{zp} Z_p &= F_z \\ J_p \ddot{\theta}_p &= T_p - F_z r_p \\ m_g \ddot{X}_g + c_{xg} \dot{X}_g + k_{xg} X_g &= -F_x \\ m_g \ddot{Y}_g + c_{yg} \dot{Y}_g + k_{yg} Y_g &= -F_y \\ m_g \ddot{Z}_g + c_{zg} \dot{Z}_g + k_{zg} Z_g &= -F_z \\ J_g \ddot{\theta}_g &= -T_g + F_z r_g \end{aligned} \right\} \quad (2)$$

where  $m_p, m_g$  are concentrated mass of the main passive bevel gear,  $J_p, J_g$  are moment of inertia of the main passive bevel gear,  $c_{jp}, c_{jg}$  are shift damping coefficient of the main passive bevel gear along the  $x, y, z$  axis directions.  $T_p$  is drive torque on the gear.  $T_g$  is impedance moment on the main passive gear.  $r_p, r_g$  is bevel gear tooth width midpoint of the base circle, circle radius.

In the (2), the relative displacement  $x_n$  is introduced as a new degree of freedom, the two torsional vibration displacement  $\theta_p, \theta_g$  is eliminated, the degree of freedom of the system is reduced from 8 to 7. It is performed by the dimensional processing.

$$\left. \begin{aligned} \ddot{x}_p + 2\zeta_{xp} \dot{x}_p + 2\zeta_{hp} c_4 \dot{x}_n + k_{xp} x_p + k_{hp} \delta(x_n) &= 0 \\ \ddot{y}_p + 2\zeta_{yp} \dot{y}_p - 2\zeta_{hp} c_5 \dot{x}_n + k_{yp} y_p - k_{hp} \delta(x_n) &= 0 \\ \ddot{z}_p + 2\zeta_{zp} \dot{z}_p - 2\zeta_{hp} c_6 \dot{x}_n + k_{zp} z_p - k_{hp} \delta(x_n) &= 0 \\ \ddot{x}_g + 2\zeta_{xg} \dot{x}_g - 2\zeta_{hg} c_4 \dot{x}_n + k_{xg} x_g - k_{hg} \delta(x_n) &= 0 \\ \ddot{y}_g + 2\zeta_{yg} \dot{y}_g + 2\zeta_{hg} c_5 \dot{x}_n + k_{yg} y_g + k_{hg} \delta(x_n) &= 0 \\ \ddot{z}_g + 2\zeta_{zg} \dot{z}_g + 2\zeta_{hg} c_6 \dot{x}_n + k_{zg} z_g + k_{hg} \delta(x_n) &= 0 \\ -c_1 \ddot{x}_p + c_2 \ddot{y}_p + c_3 \ddot{z}_p + c_1 \ddot{x}_g - c_2 \ddot{y}_g - c_3 \ddot{z}_g + \ddot{x}_n + \\ 2\zeta_h c_6 \dot{x}_n + k_h c_6 f(x_n) &= f_{pm} + f_{pv} + f_e \end{aligned} \right\} \quad (3)$$

$$\begin{aligned} x_j &= X_j / b_m & y_j &= Y_j / b_m \\ z_j &= Z_j / b_m & x &= x_n / b_m \\ \omega_n &= \sqrt{k_m / m_e} & \omega_{ij} &= \sqrt{k_{ij} / m_j} \\ \zeta_{ij} &= c_{ij} / (2m_j \omega_n) & k_{ij} &= \omega_{ij}^2 / \omega_n^2 \\ \zeta_{hj} &= c_h / (2m_j \omega_n) & k_{hj} &= k_h(\tau) / (m_j \omega_n^2) \\ \zeta_h &= c_h / (2m_e \omega_n) & \tau &= \omega_n t \\ \omega_h &= \Omega_h / \omega_n & \omega_F &= \Omega_F / \omega_n \\ k_h &= \frac{\bar{k}(t)}{k_m} = 1 + \sum_{l=1}^{N_k} \frac{A_{kl}}{k_m} \cos(l\omega_h \tau + \Phi_{kl}) \\ B_j &= \frac{A_j}{m_e \omega_n^2} \\ f_{pm} &= F_{pm} / m_e b_m \omega_n^2 & f_{pv} &= F_{pv} / m_e b_m \omega_n^2 \\ f_e &= \sum_{l=1}^{N_e} \frac{A_{el}}{b_m} (l\omega_h)^2 \cos(l\omega_h \tau + \Phi_{el}) \\ i &= x, y, z & j &= p, g \end{aligned}$$

The non-analytic function  $\delta(x_n)$  is introduced to describe the actual deformation of the gear teeth with consideration of the backlash.

$$\delta(x_n) = \begin{cases} x_n(t) - b & x_n(t) > b \\ 0 & |x_n| \leq b \\ x_n(t) + b & x_n(t) < -b \end{cases} \quad (4)$$

Where, symbol  $b$  is the half of the normal mean backlash. The image of the function  $\delta(x_n)$  is shown in Figure3

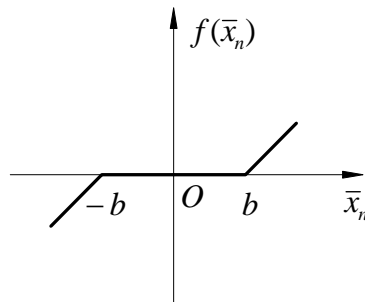


**Figure 3. The Nonlinear Backlash Function of Gear Pair**

$$f(\bar{x}_n) = \delta\left(\frac{x_n}{b}\right) = \begin{cases} \bar{x}_n(t) - 1 & \bar{x}_n(t) > 1 \\ 0 & |\bar{x}_n(t)| \leq 1 \\ \bar{x}_n(t) + 1 & \bar{x}_n(t) < -1 \end{cases} \quad (5)$$

Where  $f(\bar{x}_n)$  is comprehensive deformation of gear tooth when considering the tooth side gap

### 3. Stiffness of Gear System

In the process of gear engagement, the dynamic excitation is called the stiffness of the gear mesh, for short, because of the time varying of the rigidity of the mesh.

In the course of the engagement of the gears, the single and double teeth engage alternately. In the single tooth to the meshing area, the meshing of the gear is small, and the mesh is elastic and large. As a result, the two pairs of teeth bear the load. Therefore, the meshing of the gear is relatively large, and the mesh is small. In the process of continuous operation of the gear pair, the single and double teeth are alternately, which leads to the periodic variation of the tooth engagement. Because of the gear transmission process, the meshing stiffness is time varying, and the stiffness of the gear is periodic, so the meshing stiffness can be expanded into fourier series.

$$k_e(\bar{t}) = k_m + \sum_{j=1}^5 a_j \cos j\bar{\omega}_e \bar{t} + \sum_{j=1}^5 b_j \sin j\bar{\omega}_e \bar{t} \quad (6)$$

$$\bar{\omega}_e = \frac{2\pi z_1 n_1}{60} = \frac{2\pi z_2 n_2}{60} = \frac{\pi z_1 n_1}{30} = \frac{\pi z_2 n_2}{30} \quad (7)$$

Where  $k_m$  is average mesh stiffness,  $\bar{\omega}_e$  is meshing frequency of gear pair,  $z_1$ ,  $z_2$  are the number of teeth of the main gear and the number of passive gear teeth,  $n_1$ ,  $n_2$  are drive gear and passive gear speed. When the nonlinear describing function is fitted by the 7 degree polynomial, the dynamic equation of the gear system is obtained according to the formula (3).

$$\left. \begin{aligned}
 \ddot{x}_p + 2\zeta_{xp}\dot{x}_p + 2\zeta_{hp}c_4\dot{x}_n + k_{xp}x_p + bk_{hp}(a_1\bar{x}_n + a_3(\bar{x}_n)^3 + a_5(\bar{x}_n)^5 + a_7(\bar{x}_n)^7) &= 0 \\
 \ddot{y}_p + 2\zeta_{yp}\dot{y}_p - 2\zeta_{hp}c_5\dot{x}_n + k_{yp}y_p - bk_{hp}(a_1\bar{x}_n + a_3(\bar{x}_n)^3 + a_5(\bar{x}_n)^5 + a_7(\bar{x}_n)^7) &= 0 \\
 \ddot{z}_p + 2\zeta_{zp}\dot{z}_p - 2\zeta_{hp}c_6\dot{x}_n + k_{zp}z_p - k_{hp}(a_1\bar{x}_n + a_3(\bar{x}_n)^3 + a_5(\bar{x}_n)^5 + a_7(\bar{x}_n)^7) &= 0 \\
 \ddot{x}_g + 2\zeta_{xg}\dot{x}_g - 2\zeta_{hg}c_4\dot{x}_n + k_{xg}x_g - k_{hg}(a_1\bar{x}_n + a_3(\bar{x}_n)^3 + a_5(\bar{x}_n)^5 + a_7(\bar{x}_n)^7) &= 0 \\
 \ddot{y}_g + 2\zeta_{yg}\dot{y}_g + 2\zeta_{hg}c_5\dot{x}_n + k_{yg}y_g + k_{hg}(a_1\bar{x}_n + a_3(\bar{x}_n)^3 + a_5(\bar{x}_n)^5 + a_7(\bar{x}_n)^7) &= 0 \\
 \ddot{z}_g + 2\zeta_{zg}\dot{z}_g + 2\zeta_{hg}c_6\dot{x}_n + k_{zg}z_g + k_{hg}(a_1\bar{x}_n + a_3(\bar{x}_n)^3 + a_5(\bar{x}_n)^5 + a_7(\bar{x}_n)^7) &= 0 \\
 -c_1\ddot{x}_p + c_2\ddot{y}_p + c_3\ddot{z}_p + c_1\ddot{x}_g - c_2\ddot{y}_g - c_3\ddot{z}_g + \ddot{x}_n + 2\zeta_h c_6 \dot{x}_n & \\
 + (1 + \sum_{j=1}^5 B_j \cos(j\bar{\omega}_e \bar{t} + \phi_j))c_6(a_1\bar{x}_n + a_3(\bar{x}_n)^3 + a_5(\bar{x}_n)^5 + a_7(\bar{x}_n)^7) &= f_{pm} + f_{pv} + f_e
 \end{aligned} \right\} (9)$$

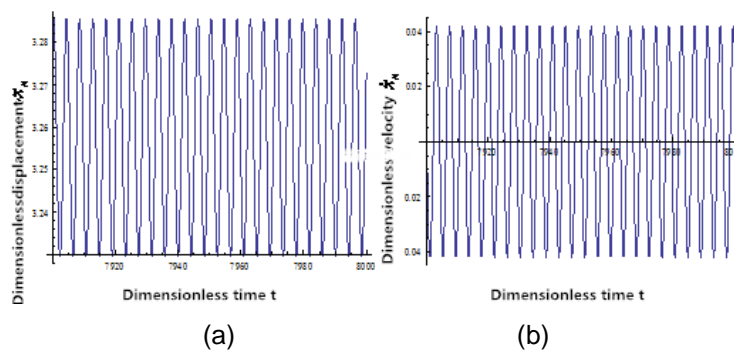
#### 4. Numerical Calculation of Mechanical Equation of Gear System

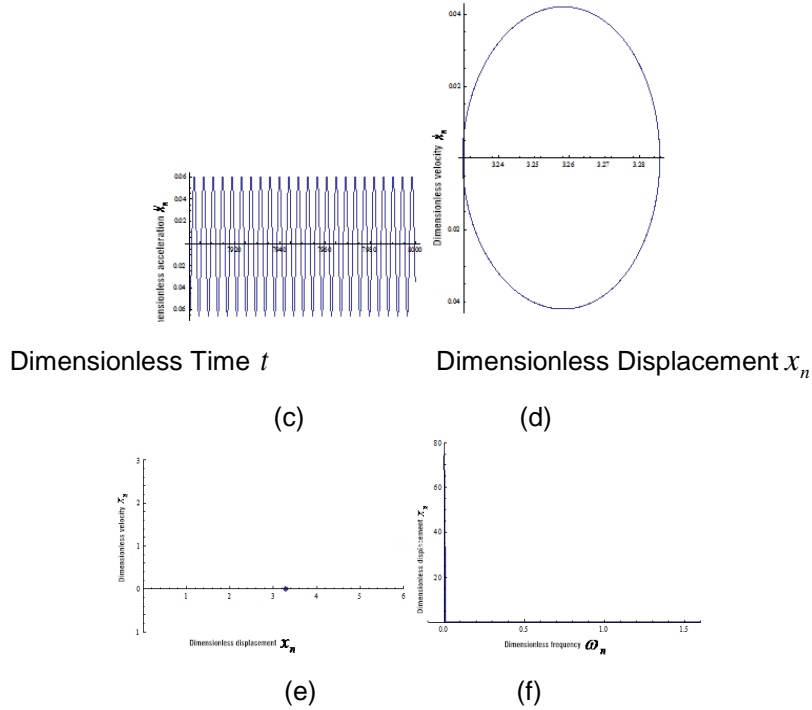
Since the differential equation (9) of the gear set up in front is a non dimensional mathematical expression, the formula (9) does not depend on the specific physical dimension, but only has the characteristics of the mathematical form. So the analysis of the characteristics of gear dynamics (9) is more extensive and representative.

In order to verify the validity of the numerical method, the arc tooth bevel gears in the RV reduction device of the micro adjustable gap variable thickness gear with the micro adjustable gap is verified. Using the above numerical simulation algorithm and the FFT algorithm, the Poincare algorithm and the spectrum of the spectrum are simulated and calculated. When calculating the driving torque and load torque are stable,

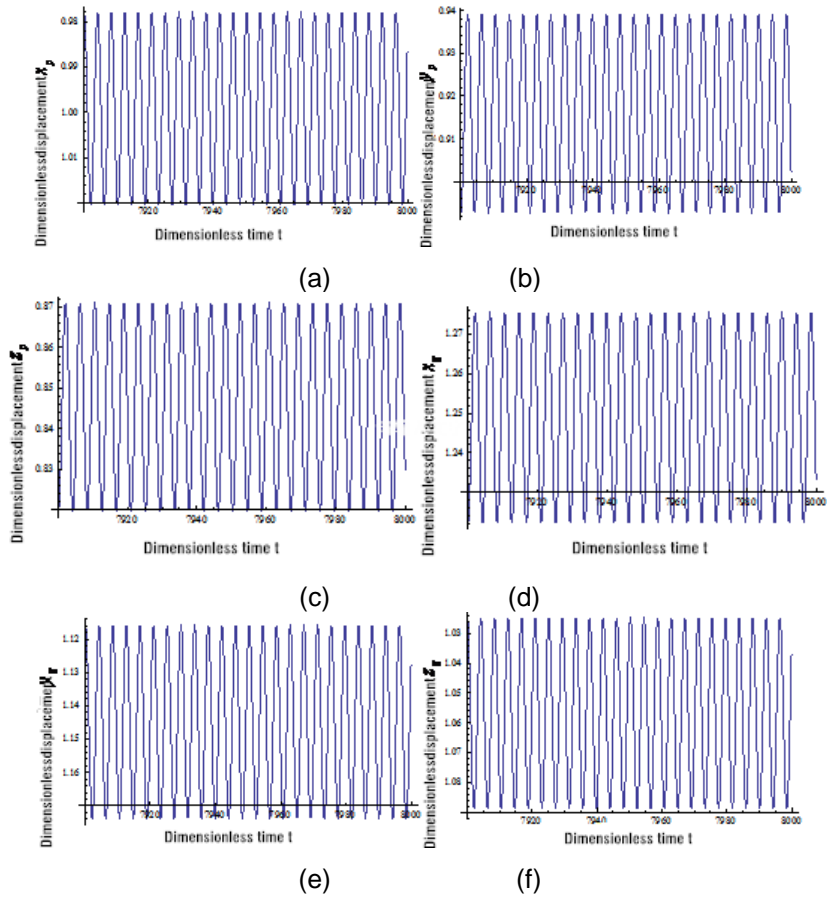
$$\begin{aligned}
 f_{lv} = 0, f_{lm} = 0.15, \phi_k = 0, \zeta_{xp} = 0.01, \zeta_{yp} = 0.015, \zeta_{zp} = 0.02, \zeta_{xg} = 0.01, \\
 \zeta_{yg} = 0.015, \zeta_{zg} = 0.02, \zeta_{hp} = 0.0125, \zeta_{hg} = 0.0125, \zeta_h = 0.04, k_{xp} = 1.1, \\
 k_{yp} = 1.2, k_{zp} = 1.3, k_{xg} = 1.1, k_{yg} = 1.2, k_{zg} = 1.3, k_{hp} = 0.4, k_{hg} = 0.5, \\
 k_h = 1 + 0.2\cos(\omega_h t), f_{pm} = 0.5, f_{pv} = 0, f_e = 0.1 \cdot \omega_h^2 \cos(\omega_h t)
 \end{aligned}$$

With the change of meshing frequency, the arc tooth bevel gear system shows rich vibration characteristics. From figure 4, the excitation frequency is  $\omega_h = 1.5$ , The response of the system is a single cycle harmonic response, with the same characteristics of the linear system, namely single frequency single frequency response. The time course of the response of the vibration displacement is a simple harmonic, and the response of the phase plane is oval. The Poincare map is a single discrete point. Figure 5 (a), (b), (c), (d), (e), (f) respectively are  $x_p$ 、 $y_p$ 、 $z_p$ 、 $x_g$ 、 $y_g$ 、 $z_g$  the relationship chart of the six non dimensional displacement and time.

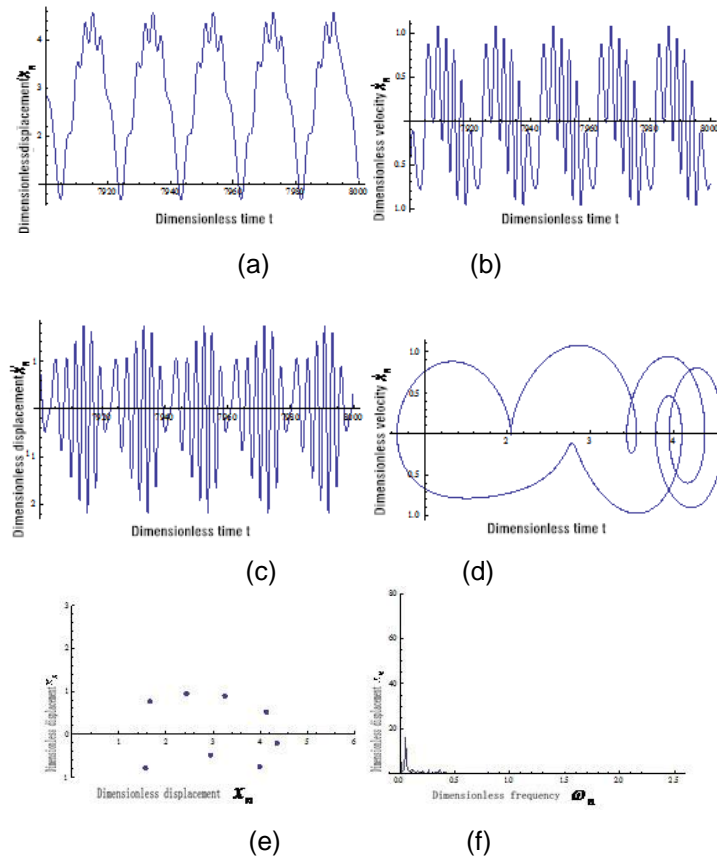




**Figure 4.**  $x_n/t, \dot{x}_n/t, \ddot{x}_n/t$ , Phase Plane Plot, Poincare & Frequency Response

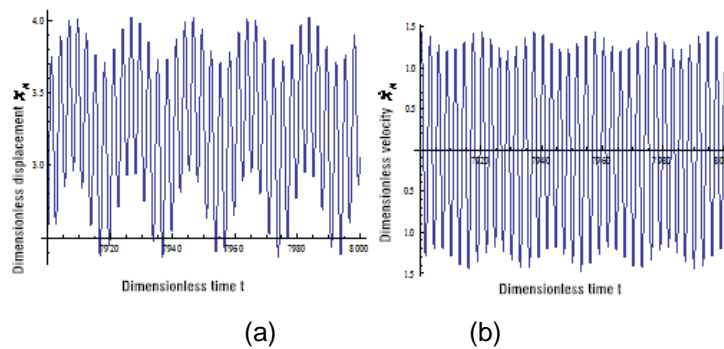


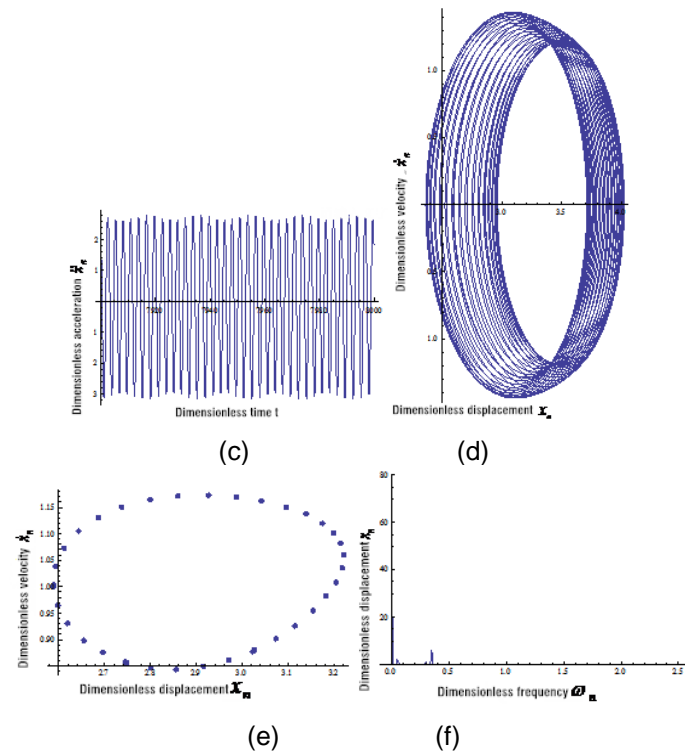
**Figure 5.** The Relation between  $x_p/t, y_p/t, z_p/t, x_g/t, x_g/t, z_g/t$



**Figure 6.**  $x_n/t, \dot{x}_n/t, \ddot{x}_n/t$ , Phase Plane Plot, Poincare & Frequency Response

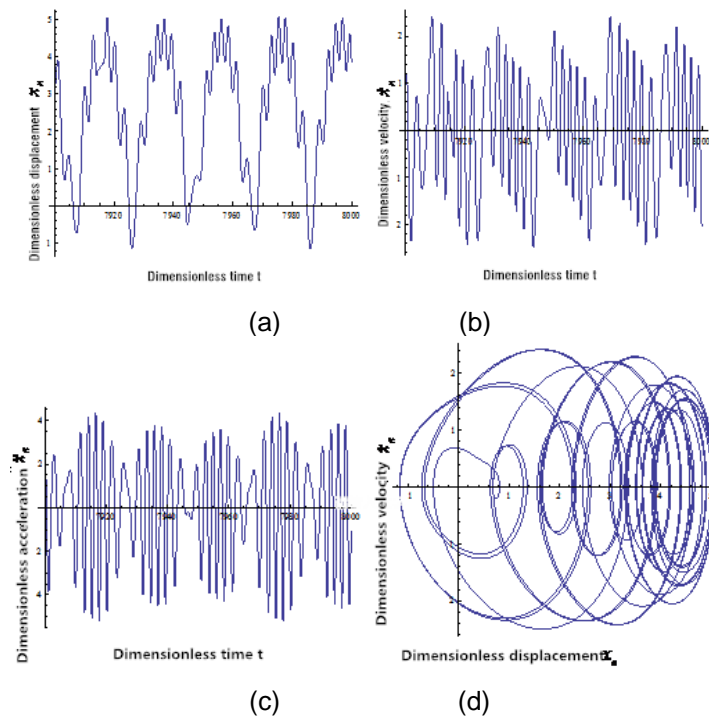
By Figure 6,  $\omega_h = 1.96$ , the system has 8 periodic harmonic response, the response is periodic motion, the corresponding phase diagram is a non circle curve, The Poincare map is 8 discrete points. Spectral lines of the FFT spectrum are scattered on the point  $m \cdot \omega_h / 8$ .





**Figure 7.  $x_n/t, \dot{x}_n/t, \ddot{x}_n/t$ , Phase Plane Plot, Poincare & Frequency Response**

By Figure 7,  $\omega_h = 2.2$ , The system appears to be periodic response, in response to the periodic motion, the motion is a combination of two or more cycles, there is no minimum period, the corresponding phase plane diagram is filled with a certain area of curve. The FFT Poincare map is a broken ring, and the spectral line of the spectrum of the spectrum is still scattered at the point of the combination frequency.



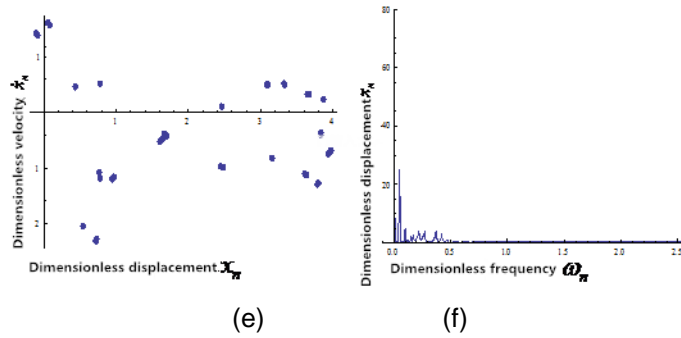


**Figure 8.**  $x_n/t, \dot{x}_n/t, \ddot{x}_n/t$ , Phase Plane Plot, Poincare & Frequency Response

By Figure 8,  $\omega_h = 2.3$ , The system appears to be in the chaotic state by the quasi periodic response, and the response of the periodic motion and the other part is an obvious chaotic state. The motion is a combination of two or more cycles, and there is no minimum period, and the spectral line of FFT spectrum is still scattered in the combination frequency.

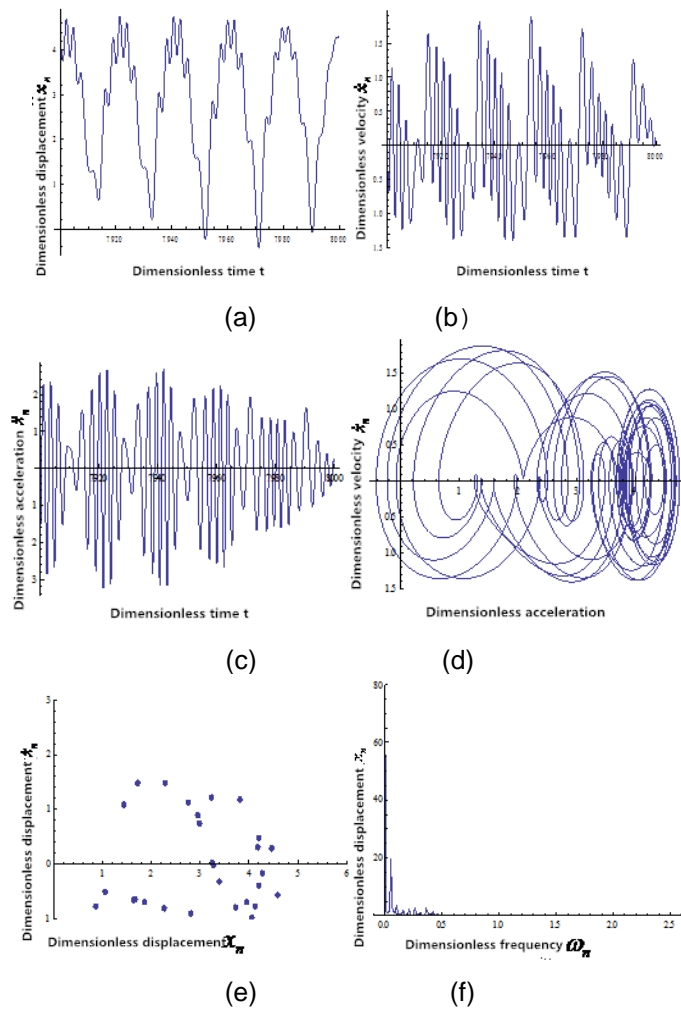


**Figure 9.**  $x_n/t, \dot{x}_n/t, \ddot{x}_n/t$ , Phase Plane Plot, Poincare & Frequency Response

By Figure 9,  $w_h = 2.5$ , The chaotic response of the system, the response is non periodic motion, the phase plane graph is composed by the mutual winding and the cross but not repeat not closed curve, Poincare and the map of the map is located in a certain region of the point set.

In the process of changing the excitation frequency, there are 2, 4, 8 periodic responses and the quasi periodic and chaotic response. The quasi periodic response is usually achieved by the quasi periodic motion. These characteristics have a great influence on the contact stability and reliability of the arc tooth bevel gear. In the design of transmission system, the value of the corresponding parameters should be avoided in the transmission system is in a chaotic response state.

## 5. Conclusion

The comprehensive analysis of the system dynamic response, including Dynamic response time history, phase diagram, Poincare map and FFT chart, shows that the exciting frequency is changed, the system appears a variety of steady state response results, namely single cycle harmonic response, response times sub-harmonic periodic, quasi periodic and chaotic response, the periodic response of the transition is by the quasi periodic bifurcation to achieve. These characteristics have great influence on the contact stability and reliability of the tooth surface of the spiral bevel gear. In the design of transmission system, the value of the corresponding parameters should be avoided in the transmission system is in a chaotic response state.

## Acknowledgment

This work supported by the Key Program of National Natural Science Foundation of Heilongjiang (Grant No. ZD201309), and Supported by Heilongjiang Natural Science Funds for Distinguished Young Scholar (Grant No. JC2015013 JC2014020), and Project supported by the Maor International Joint Research Program of China (Grant No. 2013DFA71120), and . Supported by Harbin Natural Science Funds for Distinguished Young Scholar (Grant No. 2015RAYXJ001), Professor Yu Guangbin as the corresponding author supervised this paperwork is also appreciated.

## References

- [1] G. H. Cylko, "Gears: An Alternative in Mechanical Power Transmission", Journal of Gear Technology, vol. 13, (1996), pp. 26-31.
- [2] F. Litvin, Y. Zhang, J. Wang, R. Bossler and Y. Chen, "Design and Geometry of Face-Gear Drives", ASME Journal of Mechanical Design, vol. 114, (1992), pp. 642-647.
- [3] F. Litvin, A. Egelja, J. Tan and G. Heath, "Computerized Design, Generation and Simulation of Meshing of Orthogonal Offset Face-gear Drive with a Spur Involute Pinion with Localized Bearing Contact", Mechanism and Machine Theory, vol. 33, (1998), pp. 87-102.
- [4] F. Litvin, G. Argentieri, M. De Donno and M. Hawkins, "Computerized Design, Generation and Simulation of Meshing and Contact of Face Worm-Gear Drives", Computer Methods in Applied Mechanics and Engineering, vol. 189, (2000), pp. 785-801.
- [5] T. J. Lin, and X. T. Ran, "Nonlinear vibration characteristic analysis of a face-gear drive", Journal of vibration and shock., vol. 31, no. 2, (2012), pp. 25-31.
- [6] H. X. Wang, Y. Hou and R. P. Zhu, "Tooth Surface Equations of Non-orthogonal Face Gear and Simulation", Jiangsu Machine Building & Automation, vol. 38, no. 1, (2009), pp. 94-97.
- [7] Z. Yang, S. M. Wang, Y. S. Fan and H. X. Liu, "Nonlinear dynamics of face-gear transmission system", Journal of Vibration and Shock, vol. 29, no. 9, (2010), pp. 26-35.
- [8] G. B. Yu, J. M. Wen, G. X. Li and X. Cao, "Gear method for solving dynamics differential equations of gear systems", CIMCTC'2007. Chengdu, Sichuan, China. June, 2007. Chinese Journal of Scientific Instrument, vol. 4, (2007), pp. 598-600.
- [9] R. P. Zhu and D. P. Gao, "Study on the Method of Avoiding Dedendum Undercutting and Addendum Pointing in Face Gear Design", China Mechanical Engineering, vol. 10, no. 11, (1999), pp. 1274-1276.